On the mechanisms of spontaneous growth of III-nitride nanocolumns by plasma-assisted molecular beam epitaxy

Jelena Ristić , Enrique Calleja , Sergio Fernández-Garrido , Laurent Cerutti , Achim Trampert , Uwe Jahn , Klaus H. Ploog

Ecole Polytechnique Fédérale de Lausanne (EPFL), IPEQ, Lausanne, Switzerland
ISOM and Dpt. Ingeniería Electrónica, ETSIT, Univ. Politécnica de Madrid, Spain
IES-CNRS, UMR5214, Universite de Montpellier, Montpellier, France
Paul-Drude-Institut für Festköperelektronik, Berlin, Germany

A B S T R A C T

A study of the GaN nanocolumns nucleation and growth by molecular beam epitaxy on Si(111) is presented. Ga droplets with different diameters (340–90 nm) were deposited on the substrate, prior to growth, to determine any effect on the nanocolumns size and distribution. Results indicate that there is no difference in nanocolumnar size and density whether Ga droplets are used or not, meaning that Ga droplets do not act as catalysts for the nanocolumns nucleation. In addition, Ga droplets were never observed on the nanocolumn tips upon growth termination. These findings rule out the *vapor–liquid–solid* mechanism. Instead, driven by a strong lattice mismatch nanocolumnar nucleation occurs spontaneously by Volmer–Weber growth mechanism, whereas nitrogen excess prevents the nucleation sites coalescence. Further nanocolumnar growth proceeds by direct Ga incorporation on the nanocolumns top and by Ga diffusion along the nanocolumns sidewalls up to their apex. Related to this diffusion mechanism, we found that Ga droplets, when used, may act as reservoirs to feed Ga atoms to the neighboring nanocolumns. Nanocolumns preserve a constant diameter if growth conditions are not modified because of a strong metal ad-atom diffusion length along their sidewalls. The effect of using AlN buffer layers on the nanocolumnar growth and morphology is also addressed.

Keywords:
A1. Low-dimensional structures
A1. Nanostructures
A2. Growth models
A3. Molecular beam epitaxy
B1. Nitrides
B2. Semiconducting III–V materials

1. Introduction

Even though spontaneous growth of GaN nanocolumns has been achieved by a number of groups using molecular beam epitaxy (MBE) little is still known about the mechanism behind this peculiar growth mode that, as has been shown, does not require catalyst, but only adequate growth conditions, namely the III/V ratio and growth temperature. The understanding of this growth mechanism is essential to control the nanocolumns diameter, density, and distribution, and also to achieve nanocolumnar growth on different substrates and buffer layers, avoiding the simultaneous appearance of rough compact layers (so-called "faceted matrix") and nanocolumns

The growth of Si whiskers or III–V nanocolumns was generally attributed to a *vapor–liquid–solid* (VLS) process. According to it, Si whiskers grow from Si:Au liquid droplets that are preferential sites for Si atoms incorporation from the vapor phase. The droplet, whose diameter roughly determines that of the whisker, remains generally at the whisker top upon growth termination, unless its full consumption stops the growth earlier. The droplet formation is compulsory to grow the whisker by VLS, as recently shown by Hannon

The spontaneous growth of In(Ga)N and Ga(Al)N nanocolumns by plasma-assisted MBE (PAMBE) without the help of metal catalysts (Ni or Au) on a wide variety of substrates, either buffered or bare cannot be explained in terms of a VLS process. Guha suggested that a *selective-area growth* on GaN islands, formed upon nitridation of Ga droplets, was responsible for the MBE growth of nanocolumns on Si substrates. However, the lack of detail on the growth conditions and on the size and density of the "seeding" Ga droplets or GaN

islands prevents us from drawing conclusions on whether the nanocolumns actually grew on and only on these nucleation sites. Calleja et al. suggested that Ga droplets could act as catalysts, the idea behind this suggestion being that *very small* Ga droplets ("*clusters*") formed spontaneously at the nucleation stage, could promote the nanocolumns growth in a similar way as that proposed by Guha

This work presents the study of the spontaneous nucleation and growth mechanisms of GaN nanocolumns on Si(111) substrates, though conclusions that will be drawn may apply to other III-nitride nanocolumns and substrates. The effect of Ga droplets pre-deposited on the substrate ("*droplet-patterned substrates*") on the nanocolumns nucleation process, as well as on their size, density, and distribution is addressed. Should the VLS mechanism be responsible for the GaN nanocolumnar growth under these conditions, the Ga droplets would act as preferential nucleation sites, giving rise to localized growth of nanocolumns with similar diameters as that of the droplets. New experimental results are presented and discussed, providing hints to clarify how nucleation occurs; how the nanocolumns grow; and how to avoid the simultaneous appearance of nanocolumnar and compact morphologies. All samples used for droplet-patterned experiments were grown on bare Si(111) substrates to avoid potential effects of buffer morphology, thickness, strain differences, or crystalline quality on the nucleation process.

2. Experimental procedure

Ga-droplet patterns were generated by exposing the substrate to a Ga flux at 560 °C at which Ga desorption is negligible [1]. This exposure was monitored by reflection high energy electron diffraction (RHEED) showing that the high diffraction orders vanished after 0.5 monolayers (ML) of Ga deposition [13], turning the (7×7) reconstruction into an (1×1) one. The remaining (1×1) reconstruction faded out progressively with increasing exposure to Ga until finally disappearing beyond 10 ML coverage.

The process of Ga deposition and re-evaporation (*flush-off*) to control the droplet patterning was studied by reflectivity measurements (Fig. 1). The Ga flux used was the same required to further grow the GaN nanocolumns ($\phi_{\mathrm{Ga}} = 1.7\times10^{-7}$ Torr, 0.13 ML/s). Different amounts of Ga were deposited at 560 °C and sequentially flushed-off at 700 °C. The reflectance decay time during Ga desorption at 700 °C is found to be a linear function of the Ga deposition time (Fig. 2), providing an estimate of the Ga coverage and a reproducible method for droplet patterning. Since metallic Ga forms liquid droplets on a Si surface in order to reduce the surface tension [14], droplet patterning at 560 °C as a function of the Ga coverage, from 8 to 62 ML, produced Ga droplets of different diameters and densities (see Table 1).

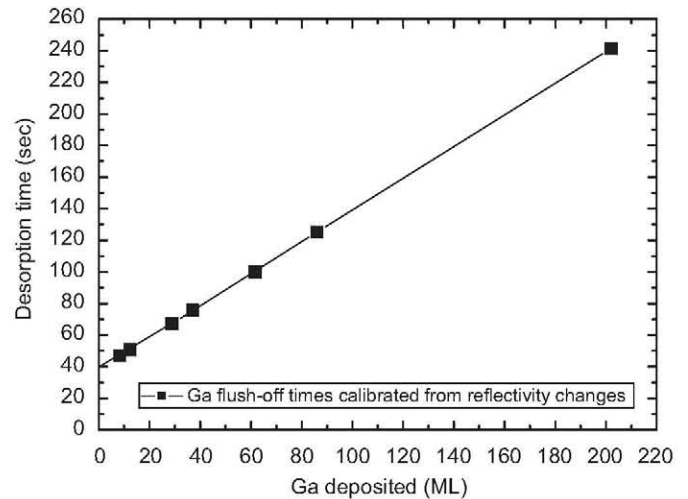

Fig. 2. Ga desorption times at 700 °C as a function of the Ga deposition times (measured in MLs), derived from experiments like those in Fig. 1. Data is taken at 700 °C.

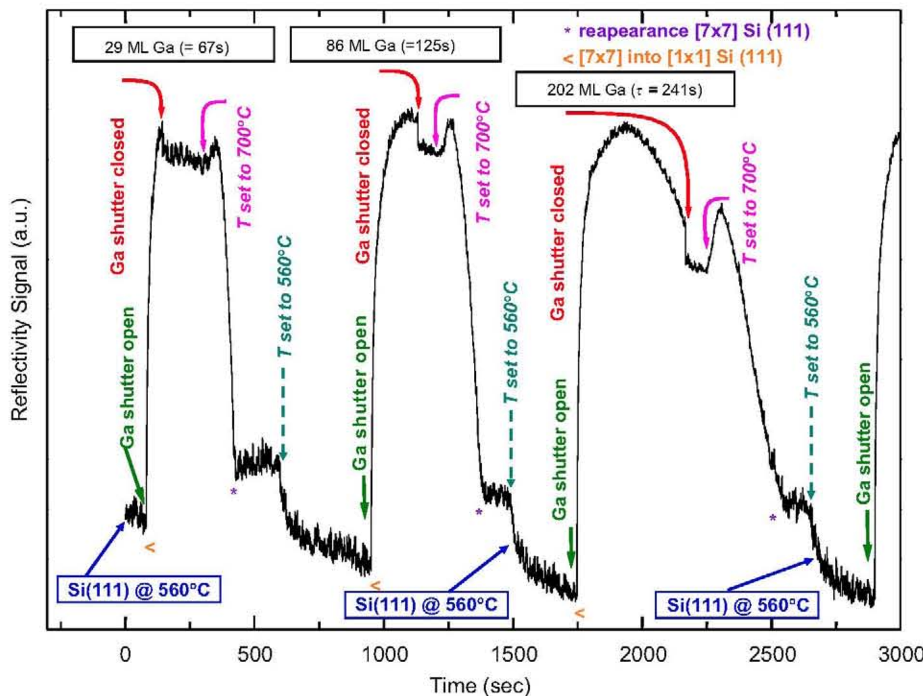

Fig. 1. Reflectivity changes during the deposition and flush-off of different amounts of Ga. (*) symbols indicate when the 7×7 Si(111) RHEED reconstruction reappears (Ga is gone), whereas (<) symbols indicate when the 7×7 turns into a 1×1 reconstruction (Ga on the surface).

Table 1
Data on the nanocolumnar samples grown (*roman values in table cells*) and on the pre-patterned substrates used (*italic values in table cells, sample names labelled with (S)*)

Sample	Deposited Ga (ML)	TDEP (°C)/ TGROWTH (°C)	Droplet (italic) or hollow (roman) diameter (μm)	Droplet (italic) or hollow (roman) density (μm^{-2})
*m*1023(*s*)	*62*	*560/–*	0.34 ± *0.05*	*1.74*
*m*1046	62	560/700	0.40 ± 0.04	0.57
*m*1058(*s*)	*12*	*560/–*	0.17 ± *0.02*	*1.57*
*m*1060	12	560/700	0.18 ± 0.04	1.03
*m*1263(*s*)	*8*	*560/–*	0.09 ± *0.02*	*1.37*
*m*1261	8	560/700	–	–
*m*1275(*s*)	*8*	*560/–*	–	–
*m*1262	8	560/700	–	–

The diameter and the density stand for droplets, in pre-patterned substrates, and for hollows between nanocolumns, in the grown samples, respectively. The nanocolumns diameter is *not* presented, being always much smaller than the Gadroplet.

Once the droplet pattern is formed at 560 °C, the substrate temperature is raised to the nanocolumnar growth value (700 °C) under continuous exposure to the N flux. Some 40 s after the temperature set-point change, the Ga cell shutter is opened and the nanocolumnar growth starts. It takes another 40 s to reach the final growth temperature (700 °C). The III/V flux ratio used for all GaN samples corresponds to that of highly N-rich growth conditions at 700 °C to ensure nanocolumnar growth regime (III/V ≈ 0.33). Even though partial Ga desorption may occur at 700 °C before the nanocolumn growth initiation, the total flush-off time for 8 ML (smallest quantity of Ga used) is about 47 s (Fig. 2). In addition, partial nitridation of the Ga droplets may take place, reducing the Ga desorption rate. Then, the temperature increase from 560 to 700 °C would not significantly affect the Ga droplet size and density from which, according to the VLS model, nanocolumnar growth should occur. A reference sample, prepared by deposition of 8 ML Ga at 560 °C, heated to reach the growth temperature of 700 °C, at the stage of the nanocolumns growth initiation (Ga cell shutter opening) presents droplets of similar size as the initially deposited ones.

Each nanocolumnar GaN sample was compared with its corresponding droplet-patterned substrate to check for possible relation between droplets and nanocolumns in terms of diameter, density, and distribution. The samples and the droplet-patterned substrates (duplicates of those used to grow nanocolumns) were studied by scanning electron microscopy (SEM). Table 1 gives details on the droplet-patterned substrates, labeled as *m*****(*s*) (italic values in table cells) and on GaN nanocolumnar samples (*m*****) (roman values in table cells).

3. Results

Sample *m*1046, grown on a substrate with Ga-droplets of 340 nm diameter (*m*1023(*s*)) reveals a homogeneous distribution of nanocolumns everywhere *but* on the original Ga-droplets sites, that appear as hollow circles (Fig. 3b) with similar diameters to those of the former Ga-droplets (Fig. 3a–c). In this case, Ga droplets seem to hinder the nanocolumn growth on them and have no relation with nanocolumns grown elsewhere.

Second sample, *m*1060 (Fig. 3e and f), was grown on a substrate with smaller (170 nm) diameter Ga droplets, *m*1058(*s*) (Fig. 3d). Results shown in Fig. 3e and f again reveal a uniform distribution of nanocolumns between the former Ga-droplet sites oriented perpendicularly to the substrate. In this case, however, there is nanocolumnar growth at the Ga droplet sites as well, though with tilted orientations with respect to the substrate (Fig. 3f). This could be interpreted as if nanocolumns emerge from the facets of partially nitrided Ga droplets, being the nitridation a process more likely to happen in the case of smaller droplets (see Fig. 4). Transmission electron microscopy (TEM) studies at early stages of the nanocolumnar growth would be required to fully ascertain this assumption. However this issue is beyond the purpose of this work.

High magnification top view SEM image of sample *m*1060 in Fig. 5 clearly shows higher density GaN of nanocolumns in the vicinity of the Ga droplet that decreases with the increasing distance from it. These results point to Ga droplets acting as reservoirs that supply Ga atoms to their close vicinity, where nanocolumns grow with a higher density. This agrees well with a kinetic nature of the nanocolumnar growth, where diffusion of Ga atoms to the nanocolum base and further to their apex plays a major role, as pointed out before by Bertness et al. [15] and Debnath et al. [16]. This point will be addressed later in more detail.

Two more GaN nanocolumnar samples were grown: first one on substrate with Ga droplets of diameter as small as 90 nm (*m*1263(*s*), in Fig. 3g) and the second on bare Si substrate, without Ga-droplets (*m*1275(*s*), in Fig. 3j). Results from SEM measurements in Fig. 3i and k are most clarifying: in both samples GaN nanocolumns grow everywhere with identical shape, size, density, orientation, and distribution. These facts are in contradiction with the VLS mechanism that does not establish a size limit for the catalyst droplet to develop into a nanocolumn [6–10]. We can thus conclude that there is no correlation between the Ga droplets and the GaN nanocolumns, whose density is always much higher (and independent) than that of the Ga-droplets.

4. Model

The study of the mechanisms behind the spontaneous growth of GaN nanocolumns addresses to two different but connected aspects: (i) the nucleation process that determines the average nanocolumn size and density; and (ii) the growth process that gives rise to nanocolumns with constant diameter. The spontaneous nucleation of GaN nanocolumns must arise from a random distribution of small GaN islands (we avoid to call them "droplets").

In order to better understand how the nanocolumns nucleation proceeds it is worth to remind how GaN Quantum Dots (QDs) grow. When the growth mode changes from two dimensional (2D) to three dimensional (3D), driven by energy minimization to reduce the strain build-up in the layer QDs develop. When the grown ML accumulate strain beyond threshold, QDs are formed simultaneously on the whole substrate surface, with average sizes that depend on the number of ML grown. It is worth to remind that QDs growth is always performed under *slightly* N-rich (Stranski-Krastanov, SK), or Ga-rich (modified SK) growth conditions . When the QDs formation is done, QDs are always observed on a wetting layer.

Fig. 3. SEM images of the substrates, patterned with Ga droplets (left), and the corresponding nanocolumnar samples grown on them, either a top view (center) or side view (right). The droplet sizes of the corresponding substrates are given on each image.

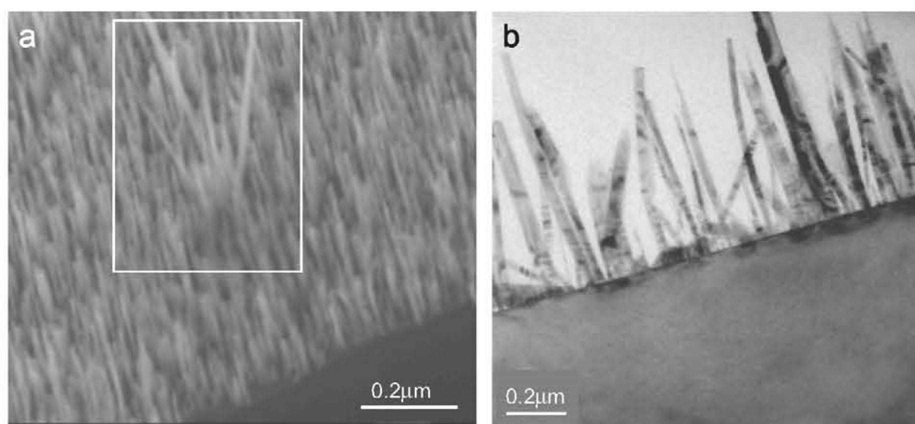

Fig. 4. (a) Detailed SEM and (b) TEM images of GaN nanocolumns growing at Ga-droplet sites, having tilted orientations (sample *m*1060 of Fig. 3e and f).

Nanocolumnar nucleation, on the other hand, does not occur suddenly over the entire substrate area, but requires some time to reach a saturation density, as shown by Calarco
These authors refer to unusually long times that are the direct consequence of the very low growth rate used. This fact does not point to a growth mode change from 2D to 3D, but instead to a direct nucleation of islands without the need of 2D growth, that is following a Volmer–Weber (VW) growth mode. This is further supported by the fact that no wetting layer has ever been observed in GaN nanocolumns neither by high resolution transmission electron microscopy (HRTEM) nor by photoluminescence (PL), even in very short nanocolumns like those shown in Fig. 6 (~30 nm high corresponding to ~8 min. growth) grown on bare Si(1 1 1), without any trace of wetting layer. The observed amorphous thin (2–3 nm) Si_xN_y layer that covers the whole substrate surface is due to the instantaneous reaction of Si when exposed to the active nitrogen plasma . Due to the different HRTEM interference patterns between GaN in [1 1 $\bar{2}$ 0] and Si in [1 1 0] projection, there is no GaN wetting layer detectable. A wetting layer, 1 ML thick, can be excluded because of the very high lattice mismatch of about 20% making it elastically unstable. The absence of wetting layer was also reported by Debnath et al.

The nucleation of thin films on a surface, from a vapor phase, generally starts by atomic condensation as 3D nuclei that eventually form a continuous film by a diffusion controlled process. According to the capillarity theory developed by Volmer and Weber, there is a critical size for these nuclei to become stable in terms of total free energy (volume and surface) [19]. Below this value, nuclei may decay either by desorption or diffusion to other nuclei. Aggregates of sizes larger than the critical one become stable deposits that keep growing by incorporation of diffusing atoms. If these critical nuclei are considered as spherical clusters, the critical radius (r) increases with the substrate temperature. These facts determine the minimum size of the nucleation sites for a given growth temperature and predict wider nanocolumn diameters when growing at higher temperatures, provided that

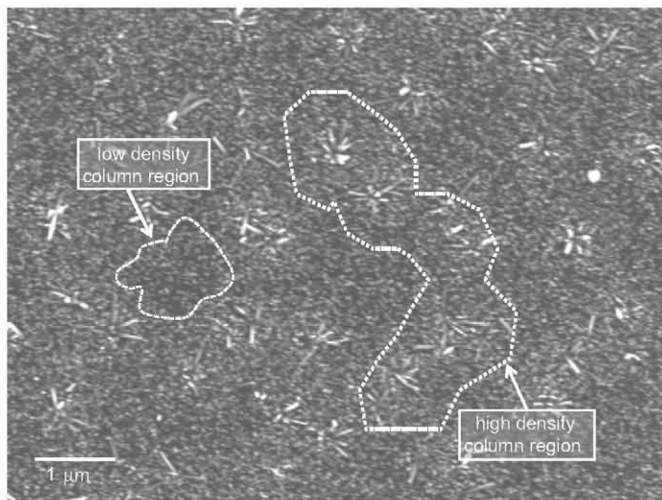

Fig. 5. Magnified SEM image of sample *m*1060, evidencing nanocolumns density fluctuations as a function of the distance from the Ga droplets.

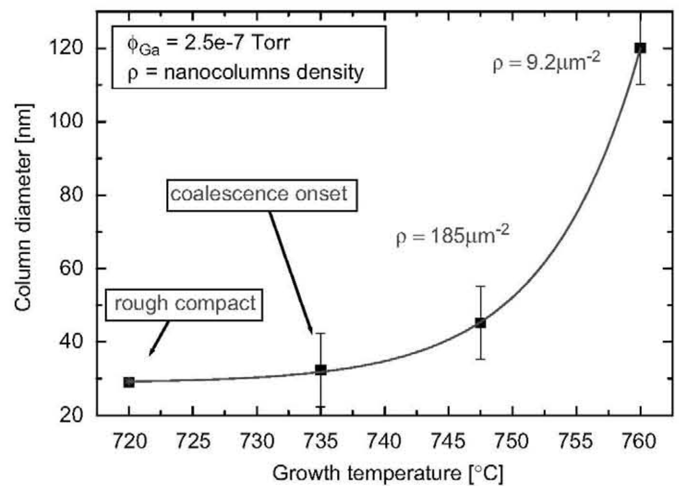

Fig. 7. Dependence of the nanocolumn diameter with the growth temperature for a given Ga flux. Notice that the measured diameters correspond to individual nanocolumns, even in cases where coalescence starts, but they are still measurable. ρ is the density of isolated nanocolumns. The symbol (*) does not correspond to nanocolumnar growth nor represents a real diameter value.

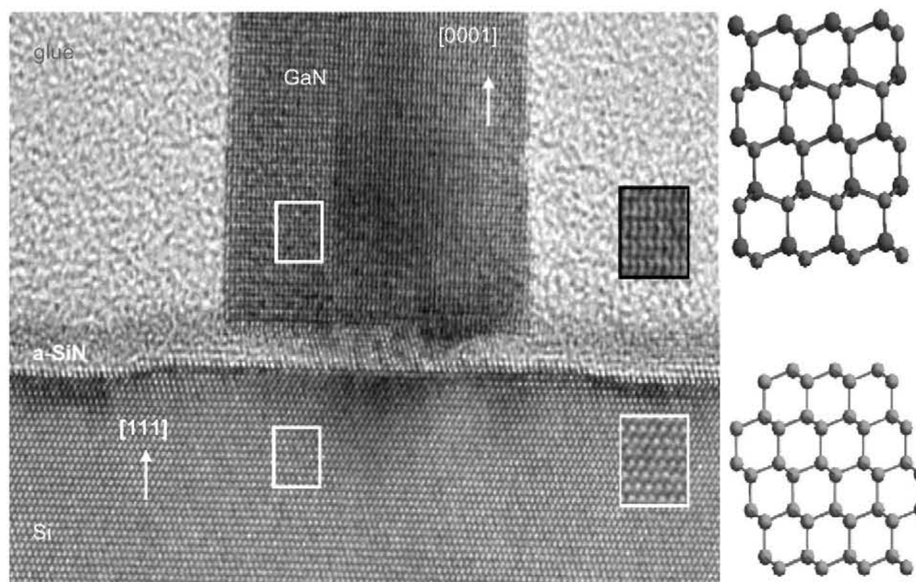

Fig. 6. HRTEM image of the interface between a GaN nanocolumn and the Si(1 1 1) substrate. A thin Si_xN_y layer is observed due to the reaction between the bare Si surface and the active nitrogen.

the Ga flux is high enough to compensate the increased desorption as is indeed observed experimentally. Fig. 7 shows the experimental dependence of the GaN nanocolumns diameter on the growth temperature.

The saturation of nucleation sites should occur when the average distance between stable nuclei equals twice the Ga ad-atoms mean diffusion length that depends both on the growth temperature and the III/V ratio. For a given growth temperature, a decrease of the III/V ratio leads to a reduction of the Ga diffusion length that determines the nanocolumn density and average diameter. When GaN is growing under extreme N-rich conditions (very small III/V ratio), stable nuclei will not coalesce because the arriving Ga ad-atoms will preferentially incorporate on their top. This preference is actually manifested by the tendency of hexagonal III-nitrides to generally grow in a columnar fashion (columnar grains). On the contrary, if Ga flux is increased (or N flux decreased) the saturation of the vertical growth will allow the onset of the lateral one, increasing the nucleation site diameter until coalescence, leading to a 2D layer morphology. This mechanism will be explained later in detail.

The fact that some time is required to reach the nanocolumns density saturation can be understood in terms of a rather small Ga diffusivity (longer time to form stable nuclei), the small Ga arriving rate (very low Ga flux to keep nitrogen excess conditions) and the decreasing probability, as the nuclei density increases to stabilize a new nucleus out of reach from other stable nuclei already existing (see diagram in Fig. 8a). The capillarity model also predicts a more favorable nucleation at surface steps because of a lower surface free energy for the formation of the nuclei.

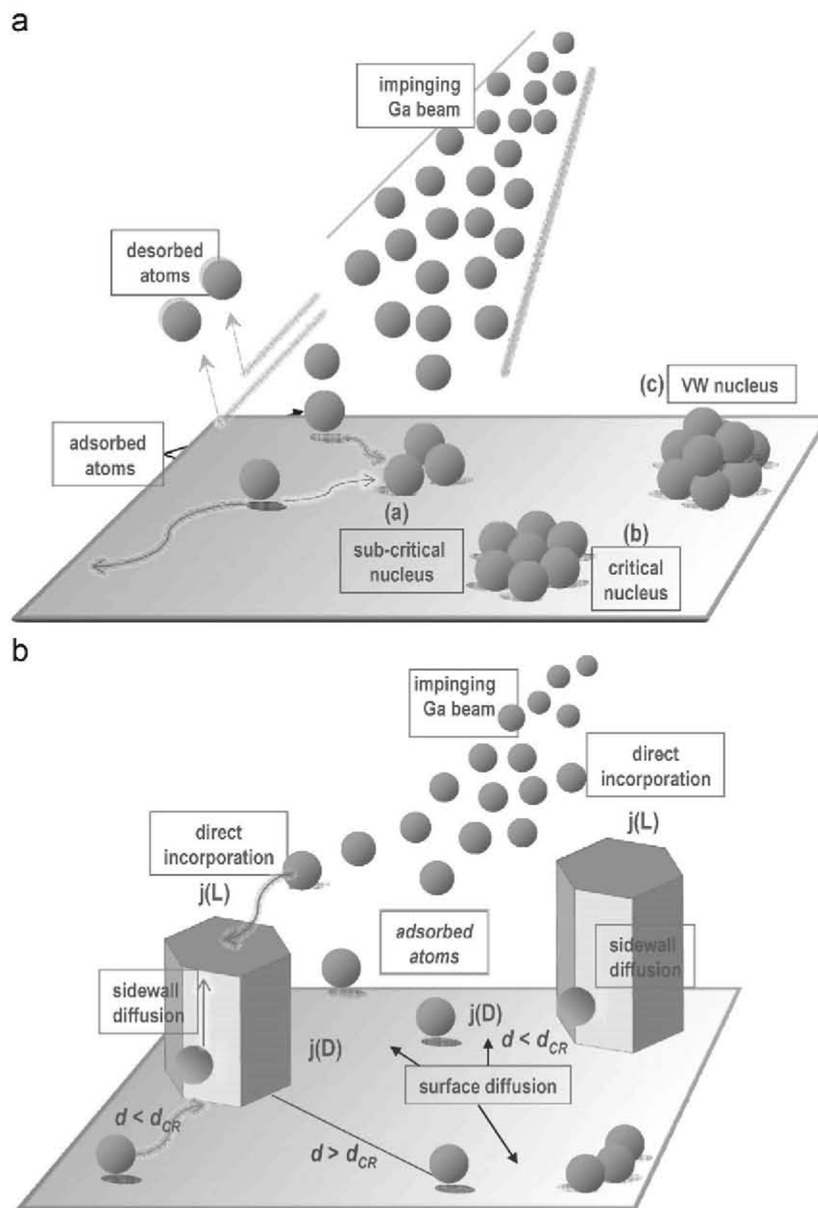

Fig. 8. (a) Diagram showing how nucleation proceeds by VB growth mode. Islands of sizes smaller than the critical one may vanish due to Ga diffusion to other stable nuclei; (b) Diagram showing how nanocolumns grow from stable nuclei. Two contributions are depicted, a direct incorporation from the impinging Ga flux (j(L)), and by Ga diffusion on the substrate (j(D)) to the nanocolumn base and up to its apex. The mean distance between nanocolumns is given by twice the average diffusion length of Ga ad-atoms. The distance dCR represents the average (critical) distance from where Ga ad-atoms can reach the nanocolumn base that depends strongly on the growth temperature.

The above model was developed to study the critical nucleus for metal films. When it comes to consider the growth of semiconductor layers on hetero-substrates, an additional factor has to be taken into account, namely, the elastic relaxation of strain. Strain relaxation depends on the cluster surface to volume ratio and some corrections must be considered to determine the actual critical radius for spherical clusters. However, the overall model picture also stands for hetero-epitaxial growth of semiconductor materials

A thorough description of the dependence of the growth mode in hetero-epitaxial systems on the total amount of deposited material and the lattice mismatch was given by Daruka and Barabasi by means of an equilibrium phase diagram. This diagram shows that for a given amount of deposited material, the growth mode and thus the morphology, can change from Frank–van der Merwe (FM), through SK, to VW as a function of increasing lattice mismatch. This diagram also illustrates that the nucleation of GaN nanocolumns on Si(111) proceeds via VW because of the very high lattice mismatch between GaN and Si(111). It will also help to understand the morphology changes that occur when GaN nanocolumns are grown on AlN buffers if no special care is taken to maintain the required N-excess. This point will be explained later in more detail.

In summary, the nucleation of GaN nanocolumns can be seen as a process in which a certain number of Ga and N atoms get together by diffusion reaching the critical size. This size may become larger, either at higher growth temperatures because of the increased Ga ad-atoms surface diffusion or by a substantial increase of the Ga flux (towards stoichiometry). In both cases, if the amount of active nitrogen is not high enough, a compact layer is obtained by islands coalescence. However, under extreme N-rich conditions, islands coalescence is blocked because of the preferential incorporation of metal atoms on the island top side, leading to a localized (nanocolumnar) growth on the nucleated islands. As mentioned before, an increase of the growth temperature under these conditions leads to wider nanocolumns if the Ga flux is kept high enough to balance the enhanced Ga desorption (Fig. 7) [11]. Thus, the N-excess seems to impose an energy barrier to the kinetic processes related to Ga ad-atom surface diffusion in a similar way as it was predicted for N-rich growth on GaN surfaces

During the nucleation process, the substrate surface becomes covered by GaN islands with different sizes (all are equal to or above the critical value) that yield differences in nanocolumn diameter. In addition, since the nucleation process does not occur simultaneously all over the substrate, some nanocolumns will start growing earlier than others giving way to the experimentally observed dispersion in heights. Moreover, variations in height among nanocolumns are expected due to the growth mechanism in which the Ga diffusion process along the nanocolumn sidewalls up to its apex can be a major contribution, thus, the wider the nanocolumn, the smaller its growth rate

Once a GaN island reaches its critical size and becomes stable, the nanocolumn starts to grow on it following a process that depends on two contributions, namely: (i) Ga atoms impinging on the nanocolumn apex will incorporate directly to the crystal; and (ii) Ga atoms arriving to the substrate surface will diffuse to the nanocolumns base, climb along the lateral sidewalls up to their apex and incorporate to the crystal as shown by the diagram in Fig. 8b.

There are some experimental facts that support this model. First, as observed in Fig. 5, the Ga droplets act as reservoirs of Ga atoms that diffuse to their neighborhood promoting the islands formation, thus, leading to a significantly higher nanocolumn density in the nearby. This phenomenon is related to the diffusion process of Ga atoms from the droplet during island nucleation and the subsequent nanocolumnar growth. Notice that the local III/V ratio nearby the Ga droplets, and thus the Ga diffusion length may be considerably different than further away. This may explain why the nanocolumnar density increases close to the droplets. It is worth to remark that the size of the Ga droplets in Fig. 5, considered as spheres, have a volume more than 100 times bigger than nanocolumns of the same height, thus being able to supply many of the surrounding columns. Second evidence is the fact that nanocolumns coalesce upon an increase of Ga flux, because their diameter becomes larger just at their top side and not all along their sidewalls This fact is interpreted as a strong increase of the density of Ga atoms that diffuse along the nanocolumns sidewalls, yielding a significant Ga accumulation at the nanocolumn topmost region. This accumulation means that not all Ga atoms can be incorporated into the crystal at the nanocolumns top since the growth rate is limited, but instead their stagnation (long residence time) allows their incorporation at the lateral sidewalls giving rise to an increase of diameter. It has been observed experimentally that the diameter increase is continuous with time until the nanocolumns' merging is reached (Fig. 9). Similar findings are reported

The issue that is so far still not explained is that the nanoclumns preserve constant diameter, provided that the growth conditions (N and Ga fluxes, and growth temperature) are kept constant during growth. A rather phenomenological explanation of the growth rate anisotropy assumes strong differences of the

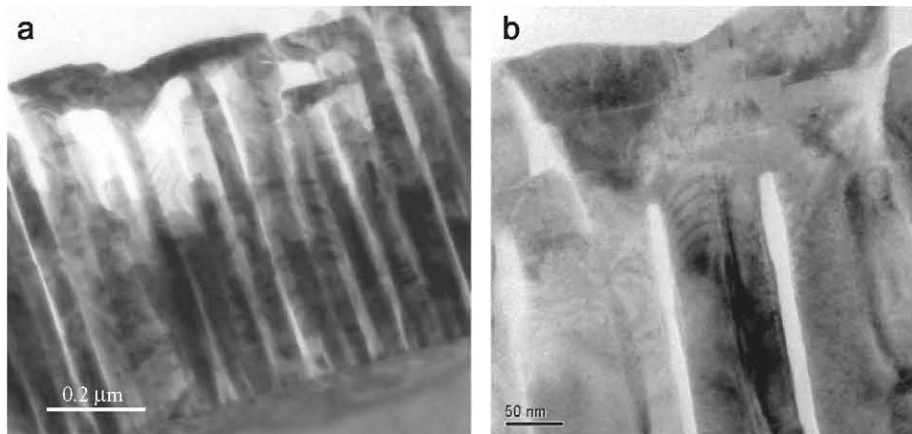

Fig. 9. Detailed SEM images of: (a) merging InGaN nanocolumns when increasing the metal flux, and (b) merging GaN nanocolumns when doping with Mg.

chemical potential or the sticking coefficient between nanocolumn sidewalls and its tip. Another viewpoint considers a very high Ga (metal) diffusion length along the nanocolumns sidewalls (in our case, m-plane facets) because of their specific surface reconstruction. Indeed, this second suggestion agrees with the already mentioned Ga diffusion process along the nanocolumn sidewall. The diffusion length (Λ), given by expression (1), depends on the average jump distance (a) between adsorption sites at the surface, the ad-atom desorption energy (Q_{des}), and the activation energy (potential well) for a surface diffusion jump (Q_d)

$$\Lambda = \sqrt{2}a \exp\left(\frac{Q_{des} - Q_d}{2kT}\right) \quad (1)$$

Atomically flat nanocolumn sidewalls, with ideal surface reconstructions, may provide few adsorption sites, far from each other, characterized by rather small Q_d values. Since Q_{des} is fixed for a given surface, ad-atom, and temperature, the diffusion length on such a surface should be quite high, resulting in a rather short time for the ad-atoms to incorporate into the crystal. On the other hand, Ga ad-atoms on the c-plane surface (nanocolumn top), which is the nanocolumns' main growth front, must have a much lower diffusion length due to the availability of more ad-atom adsorption sites with higher Q_d values (higher number of free bonds). Actually, the number of dangling bonds that relate to the ad-atom trapping is larger on c-planes than on m-planes. In addition, the surface energies, which directly affect the growth rates, are of some 120 meV/Å^2 on a- and m-plane, and about 185 meV/Å^2 on c-plane facets under N-rich growth conditions This picture may explain the strong growth rate anisotropy between the nanocolumn top and sidewalls.

As mentioned before, it was experimentally observed that an increase of the III/V ratio during the nanocolumn growth leads to coalescence at the nanocolumns topmost region because their diameter increases. This is a result of a change in the vertical to lateral growth rate anisotropy, but localized in the nanocolumns topmost region. Aside from being an evidence of the Ga ad-atoms diffusion along the nanocolumns sidewalls, this diameter increase can be understood as a consequence of an accumulation of Ga atoms and, thus, their much longer residence time that eventually leads to incorporation into the crystal at the sidewalls upper region. Fig. 9a shows the coalescence effect in InGaN nanocolumns grown on Si(111), when the metal flux is increased. A similar effect is also observed when the metal flux is kept constant but the nanocolumn is p-doped with Mg (Fig. 9b). Although not directly related with our main discussion topic, it is worth to comment that Mg also induces the nanocolumn diameter increase up to coalescence, because Mg atoms enhance the residence time of the Ga atoms, thus, allowing for a more efficient incorporation to the crystal

When Ga(Al)N nanocolumns are grown on AlN buffered Si(111) a mixture of rough-compact areas ("faceted matrix") and nanocolumns is often observed. A recent work on GaN nanocolumns grown on low-temperature AlN-buffered Si(111) suggests that nanocolumns may nucleate on the deeps (craters) of the faceted matrix, or even on top of it An early evidence of such morphology was reported for AlGaN nanocolumns grown on AlN-buffered Si(111) where both AlGaN nanocolumns and the rough faceted matrix were observed. However, results from TEM analysis on this kind of samples showed that AlGaN nanocolumns nucleated on the AlN buffer surface (not on the AlGaN faceted matrix) *simultaneously* to the growth of the faceted matrix

The effect of AlN buffer on the targeted nanocolumnar morphology is shown in Fig. 10a and c that correspond to samples grown on AlN-buffered and bare Si(111) substrates, respectively,

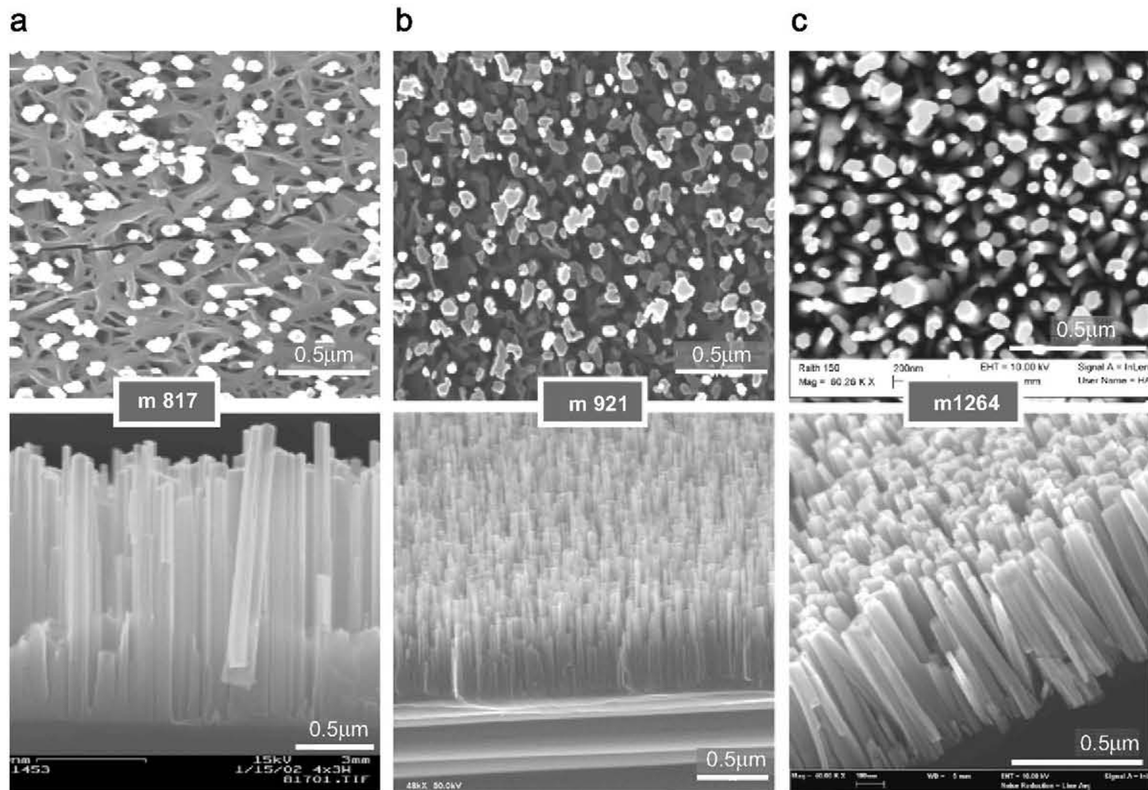

Fig. 10. Top and side SEM images of GaN nanocolumns grown at the same temperature on: (a) AlN buffered Si(111); (b) same AlN buffered Si(111) as in (a) with a higher nitrogen excess; and (c) bare Si(111) with the same III/V ratio as in (a).

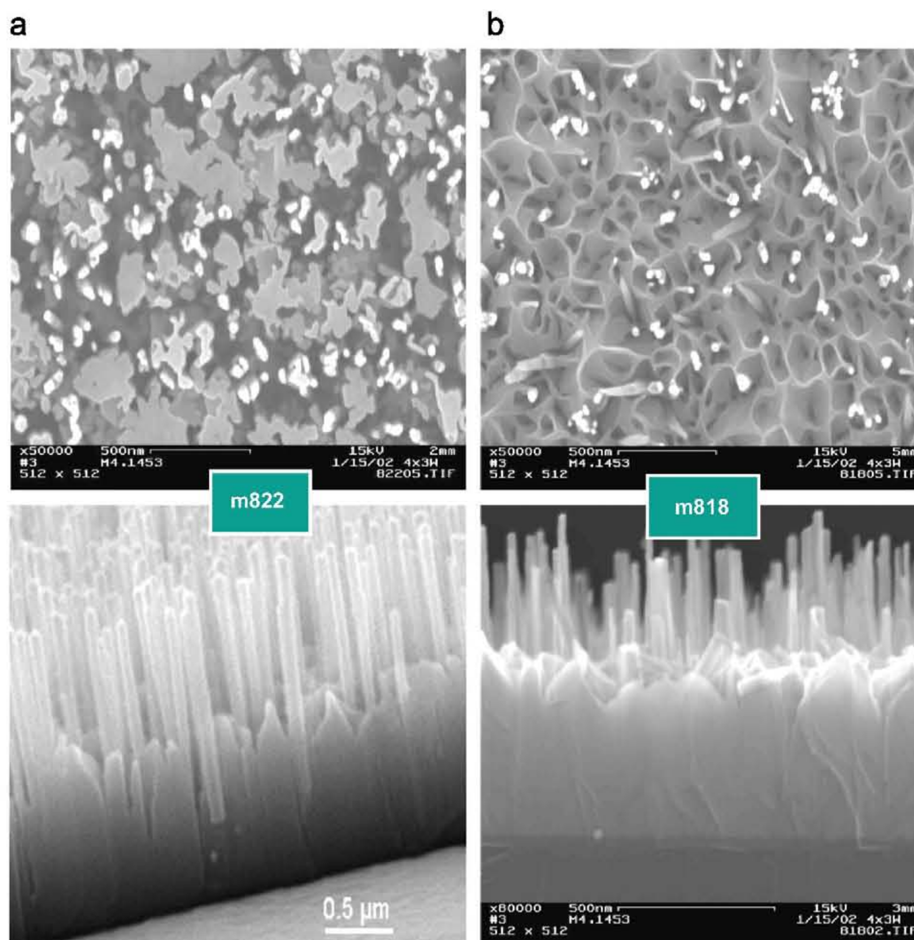

Fig. 11. Top and side SEM images of AlGaN nanocolumns on AlN buffered Si(111) with increasing III/V ratio (lower N-excess) from (a) to (b). The AlN buffer was 30 nm thick in both samples.

under the same growth conditions (III/V ratio and temperature). The appearance of the faceted matrix is evident in Fig. 10a. The origin of this faceted morphology relies on the fact that nanocolumns are not grown on bare Si(111), but on an AlN buffer layer that modifies drastically the lattice mismatch. Following the phase diagram previously mentioned a strong reduction in lattice mismatch will enable better wetting properties and promote a SK or even a FM growth mode, yielding much wider islands that will partially coalesce during the nucleation process (better wetting properties), while nanocolumns still may grow in between these islands thanks to the N-excess. Further growth of these wider, partially coalesced islands will generate enough strain as to roughen their surfaces (2D to 3D), resulting in a rough-compact material coexisting with nanocolumns. Once the AlN buffer layer is grown and the new lattice mismatch value (in respect to GaN) is settled, the Ga metal ad-atoms diffusion can still be tuned by means of the N-excess. In other words, the Ga diffusivity increase due to the lower mismatch (and the fact that Ga ad-atoms now see AlN instead of Si) can be counterbalanced by further increasing the N-excess. This is indeed what happens, as shown in Fig. 10b.

A similar trend can be observed for AlGaN nanocolumns that clearly shows how the faceted matrix develops for *standard* N-excess conditions when growing without AlN buffer (Fig. 11b), while it is very much reduced (almost gone) for higher N-excess. Notice that the N-excess has a two fold effect: one, it reduces the Ga ad-atom diffusion length on the substrate surface; and two, it favours the vertical growth on the nanocolumns top. Then, when growing nanocolumns on different substrates/buffers the N-excess has to be tuned to the appropriate value.

The last point to be addressed is the growth of nanocolumnar heterostructures, where different materials are sequentially grown while trying to keep the nanocolumnar morphology. A typical case is that of GaN/Al(Ga)N nanocavities with Bragg reflectors, like those reported In this work it was shown that the growth of the AlN region of the Bragg's AlN/GaN bilayers induced an increase of the nanocolumn diameter, even in the AlGaN barrier layers, and led to growth on the side facets of the columns in the later layers (both GaN anf AlN). Fig. 12a and b clearly show this effect that is a result of lower diffusion length of the Al ad-atoms as compared to Ga ones on the nanocolumn sidewalls, thus allowing for a higher lateral growth rate Notice that the increase of the nanocolumn diameter is not limited to the Al(Ga)N region along the nanocolumn, but also occurs further down the GaN/Al(Ga)N heterojunction. This is also shown in Fig. 12c, where an AlN nanocolumn was grown on top of a GaN one under the same conditions. Again, it is evident that the lateral growth is enhanced when AlN is grown under the same N-excess (III/V ratio) as the initial GaN nanocolumn. Recently, similar results have been reported by Calarco and by Tchernycheva estimating a 3% and 25%–35% lateral growth rates for GaN and AlN in respect to the corresponding vertical ones in AlN/GaN nanocolumnar heterostructures. The last work shows that an increase of the Ga flux in real time enhances the GaN lateral growth, in agreement with our previous comments on the nanocolumns lateral merging. It also shows that the

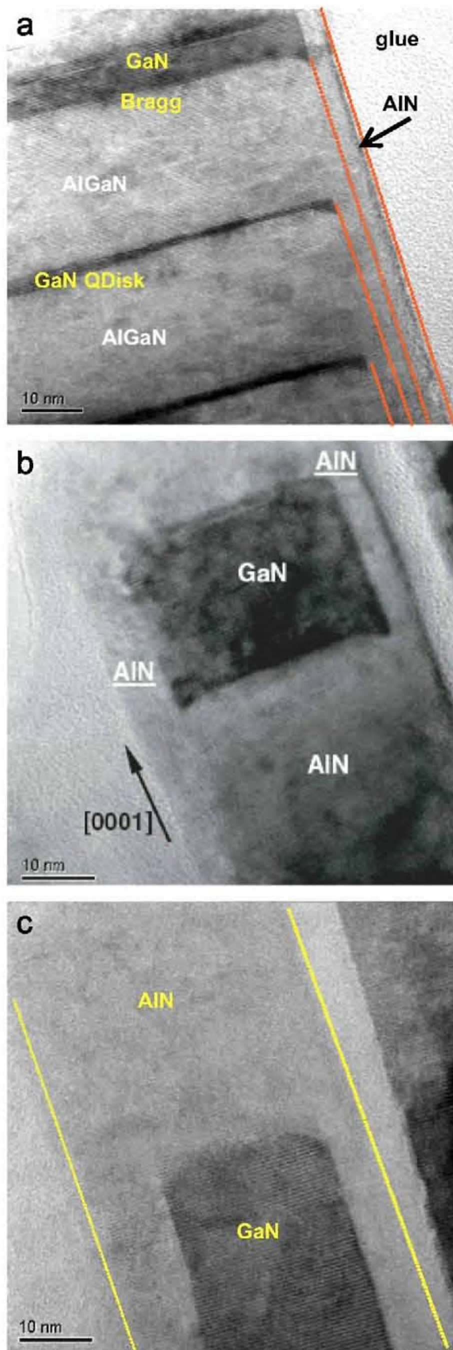

Fig. 12. HRTEM images of: (a) an AlGaN/GaN nanocolumnar heterostructure showing the enhancement of the lateral growth in Al-containing layers, as well as non-planar edges; (b) a nanocolumnar AlN/GaN Bragg reflector stack; and (c) an AlN nanocolumn grown on top of a GaN one under the same N-excess

lateral growth rate enhancement when growing AlN produces round-shaped edges, in agreement with the results reported as illustrated in Fig. 12.

5. Conclusions

In the summary, a study of the spontaneous growth of GaN nanocolumns on Si(111) substrates by molecular beam epitaxy (MBE) has been presented. Results from the nanocolumnar growth on Ga droplet-patterned substrates clearly show that the growth mechanism is not the VLS, nor it requires any seeding or catalyst at the substrate surface. Instead, when present, Ga droplets may act as reservoirs that feed with Ga ad-atoms the neighbor nucleation sites and the nanocolumn growth, pointing to a kinetic process, where diffusion of Ga atoms towards the nanocolumn apex plays an important role.

The spontaneous nanocolumnar nucleation occurs most likely by a VW growth mechanism of small islands (of critical radius or larger than) driven by the lattice mismatch with the substrate, while the excess nitrogen reduces the lateral growth rate preventing the islands coalescence. Further nanocolumnar growth proceeds by Ga incorporation directly on the nanocolumn top and by Ga diffusion along the nanocolumn sidewalls up to its apex. The nanocolumns preserve their diameter during growth because of a very high metal ad-atom diffusion length on column sidewalls. However, an increase of the Ga flux may lead to Ga accumulation at the nanocolumn topmost region resulting in an enhancement of the lateral growth rate that increases of the nanocolumn top diameter. This effect may eventually lead to the nanocolumns merging in their upper regions.

When GaN nanocolumns are grown on AlN buffer, the lattice mismatch is drastically reduced. This lattice mismatch reduction can promote a SK or even a FM growth mode that yield wider islands that partially coalesce during the nucleation process (better wetting properties), resulting in a mixture of rough-compact material (faceted matrix) and nanocolumns. A smaller III/V ratio is needed to further reduce the metal-ad-atoms diffusion rate and to avoid the appearance of the faceted matrix.

In the case of nanocolumnar heterostructures with sequential GaN/Al(Ga)N layers, the Al-containing layers induce an increase of the nanocolumn diameter, together with a non-planar (faceted) edge growth of the subsequent layers. This effect may relate to a lower diffusion length of the Al ad-atoms on the nanocolumn sidewalls as compared to Ga ones. In this case, the increase of the nanocolumn diameter is not limited to the AlN region but also happens beyond the GaN/AlN heterojunction position along the nanocolumn sidewall. In addition, when the Ga flux is increased during the nanocolumn growth, the induced lateral growth rate enhancement, by metal accumulation, leads to the nanocolums top diameter enhancement and the eventual merging. The conclusions derived from this work may apply to other III-nitride nanocolumns grown on any substrate, with or without buffer layer.

Acknowledgments

J. Ristic would like to thank Prof. Benoit Deveaud-Pledran, Prof. Nicolas Grandjean, and Dr. Pascal Gallo for valuable scientific discussion. The authors wish to acknowledge partial support by the Spanish Ministry of Education and Science, Projects NAN2004-09109-C04-02; MAT2004-02875, Consolider CSD2006-00019, FIT-330100-2007-134, and by the CAM Project (IV PRICYT) S-0505/ESP-0200.

References

M.A. Sánchez-García, E. Calleja, E. Monroy, F.J. Sánchez, F. Calle, E. Muñoz, R. Beresford, J. Crystal Growth 183 (1998) 23;
E. Calleja, M.A. Sánchez-García, F.J. Sánchez, F. Calle, F.B. Naranjo, E. Muñoz, S.I. Molina, A.M. Sánchez, F.J. Pacheco, R. García, J. Crystal. Growth 201 (1999) 296.
M. Yoshizawa, A. Kikuchi, M. Mori, N. Fujita, K. Kushi, K. Kishino, Jpn. J. Appl. Phys. 36 (1997) L459.
S. Guha, N. Bojarczuk, M. Johnson, J. Schetzina, Appl. Phys. Lett 75 (1999) 463.
R. Calarco, M. Marso, T. Richter, A.I. Aykanat, R. Meijers, A.V. Hart, T. Stoica, H. Lüth, Nanoletters 5 (2005) 981.

K.A. Bertness, A. Roshko, N.A. Sanford, J.M. Barker, A.V. Davydov, J. Crystal Growth 287 (2006) 522.
R. Wagner, W. Ellis, Appl. Phys. Lett 4 (1964) 89.
M. Koguchi, H. Kakibayashi, M. Yazawa, K. Hiruma, T. Katsuyama, Jpn. J. Appl. Phys. 31 (1992) 2061.
W. Seifert, M. Borgström, K. Depperta, K.A. Dicka, J. Johansson, M.W. Larsson, T. Martensson, N. Skölda, C.P.T. Svensson, B.A. Wacaser, L.R. Wallenberg, L. Samuelson, J. Crystal Growth 272 (2004) 211.
K. Hiruma, M. Yazawa, T. Katsuyama, K. Ogawa, K. Haraguchi, M. Koguchi, H. Kakibayashi, J. Appl. Phys. 77 (1995) 447.
J.B. Hannon, S. Kodambaka, F.M. Ross, R.M. Tromp, Nature 440 (2006) 69.
E. Calleja, J. Ristić, S. Fernández-Garrido, L. Cerutti, M.A. Sánchez-García, J. Grandal, A. Trampert, U. Jahn, G. Sánchez, A. Griol, B. Sánchez, Phys. Stat. Sol. (b) 244 (2007) 2816.
E. Calleja, M.A. Sánchez-García, F.J. Sánchez, F. Calle, F.B. Naranjo, E. Muñoz, U. Jahn, K.H. Ploog, Phys. Rev. B 62 (2000) 16826.
One ML of Ga corresponds to exposure to the amount of Ga that would result in 1 ML thick GaN under stoichiometric growth conditions ($c/2 = 0.259$ nm).
H. Luth, Surfaces and Interfaces of Solid Materials, Springer, Berlin, 1993.
K.A. Bertness, A. Roshko, L.M. Mansfield, T.E. Harvey, N.A. Sanford, J. Crystal Growth 300 (2007) 94.
R.K. Debnath, R. Meijers, T. Richter, T. Stoica, R. Calarco, H. Lüth, Appl. Phys Lett 90 (2007) 123117.
B. Daudin, F. Widmann, G. Feuillet, Y. Samson, M. Arlery, J.L. Rouviere, Phys. Rev. B 56 (1997) R7069;
N. Gogneau, D. Jalabert, E. Monroy, T. Shibata, M. Tanaka, B. Daudin, J. Appl. Phys. 94 (2003) 2254.
R. Calarco, R.J. Meijers, R.K. Debnath, T. Stoica, E. Sutter, H. Lüth, Nanoletters 7 (2007) 2248.
K. Chopra, Thin Film Phenomena, McGraw-Hill, New York, 1969.
T. Zywietz, J. Neugebauer, M. Sheffler, Appl. Phys. Lett. 73 (1998) 487;
T. Zywietz, J. Neugebauer, M. Scheffler, J. Northrup, Chris G. Van de Walle, MRS Internet J. Nitride Semicond. Res. 3 (1998) 26.
V.A. Shchukin, N.N. Ledentsov, P.S. Kopev, D. Bimberg, Phys. Rev. Lett 75 (1995) 2968.
V.A. Shchukin, D. Bimberg, Rev. Mod. Phys. 71 (1999) 1125.
I. Daruka, A.-L. Barabasi, Phys. Rev. Lett 79 (1997) 3708.
A. Kikuchi, M. Kawai, M. Tada, K. Kishino, Jap. J. Appl. Phys. 43 (2004) L1524.
J. Northrup, J. Neugebauer, Phys Rev. B 53 (1996) R10477.
J. Elsner, M. Haugk, G. Jungnickel, Th. Frauenheim, Solid State Commun. 106 (1998) 739.
K. Rapcewicz, M. Buongiorno Nardelli, J. Bernholc, Phys. Rev. B 56 (1997) R12 725.
B. Daudin, G. Mula, P. Peyla, Phys. Rev. B 61 (2000) 10330.
J. Ristic, M.A. Sánchez-García, E. Calleja, J. Sánchez-Páramo, J.M. Calleja, U. Jahn, K.H. Ploog, Phys. Stat. Sol. (a) 192 (2002) 60;
J. Ristic, E. Calleja, M.A. Sánchez-García, J.M. Ulloa, J. Sánchez-Páramo, J.M. Calleja, U. Jahn, A. Trampert, K.H. Ploog, Phys. Rev. B 68 (2003) 125305.
A. Trampert, J. Ristic, U. Jahn, E. Calleja, K.H. Ploog, Conf. Ser, in: A.G. Cullis, P.A. Midgley (Eds.), Proceedings of the 13th International Conference on Microscopy of Semiconductor. Materials, vol. 180, IOP, 2003, p. 167.
J. Ristic, E. Calleja, A. Trampert, S. Fernández-Garrido, C. Rivera, U. Jahn, K.H. Ploog, Phys. Rev. Lett 94 (2005) 146102;
J. Ristić, E. Calleja, S. Fernández-Garrido, A. Trampert, U. Jahn, K.H. Ploog, M. Povoloskyi, A. Di Carlo, Phys. Stat. Sol. (a) 202 (2005) 367.
M. Tchernycheva, C. Sartel, G. Cirlin, L. Travers, G. Patriarche, J.-C. Harmand, Le Si Dang, J. Renard, B. Gayral, L. Nevou, F. Julien, Nanotechnology 18 (2007) 385306.

chemical potential or the sticking coefficient between nanocolumn sidewalls and its tip. Another viewpoint considers a very high Ga (metal) diffusion length along the nanocolumns sidewalls (in our case, m-plane facets) because of their specific surface reconstruction. Indeed, this second suggestion agrees with the already mentioned Ga diffusion process along the nanocolumn sidewall. The diffusion length (Λ), given by expression (1), depends on the average jump distance (a) between adsorption sites at the surface, the ad-atom desorption energy (Q_{des}), and the activation energy (potential well) for a surface diffusion jump (Q_d)

$$\Lambda = \sqrt{2}a \exp\left(\frac{Q_{des} - Q_d}{2kT}\right) \quad (1)$$

Atomically flat nanocolumn sidewalls, with ideal surface reconstructions, may provide few adsorption sites, far from each other, characterized by rather small Q_d values. Since Q_{des} is fixed for a given surface, ad-atom, and temperature, the diffusion length on such a surface should be quite high, resulting in a rather short time for the ad-atoms to incorporate into the crystal. On the other hand, Ga ad-atoms on the c-plane surface (nanocolumn top), which is the nanocolumns' main growth front, must have a much lower diffusion length due to the availability of more ad-atom adsorption sites with higher Q_d values (higher number of free bonds). Actually, the number of dangling bonds that relate to the ad-atom trapping is larger on c-planes than on m-planes. In addition, the surface energies, which directly affect the growth rates, are of some 120 meV/Å^2 on a- and m-plane, and about 185 meV/Å^2 on c-plane facets under N-rich growth conditions This picture may explain the strong growth rate anisotropy between the nanocolumn top and sidewalls.

As mentioned before, it was experimentally observed that an increase of the III/V ratio during the nanocolumn growth leads to coalescence at the nanocolumns topmost region because their diameter increases. This is a result of a change in the vertical to lateral growth rate anisotropy, but localized in the nanocolumns topmost region. Aside from being an evidence of the Ga ad-atoms diffusion along the nanocolumns sidewalls, this diameter increase can be understood as a consequence of an accumulation of Ga atoms and, thus, their much longer residence time that eventually leads to incorporation into the crystal at the sidewalls upper region. Fig. 9a shows the coalescence effect in InGaN nanocolumns grown on Si(111), when the metal flux is increased. A similar effect is also observed when the metal flux is kept constant but the nanocolumn is p-doped with Mg (Fig. 9b). Although not directly related with our main discussion topic, it is worth to comment that Mg also induces the nanocolumn diameter increase up to coalescence, because Mg atoms enhance the residence time of the Ga atoms, thus, allowing for a more efficient incorporation to the crystal

When Ga(Al)N nanocolumns are grown on AlN buffered Si(111) a mixture of rough-compact areas ("faceted matrix") and nanocolumns is often observed. A recent work on GaN nanocolumns grown on low-temperature AlN-buffered Si(111) suggests that nanocolumns may nucleate on the deeps (craters) of the faceted matrix, or even on top of it An early evidence of such morphology was reported for AlGaN nanocolumns grown on AlN-buffered Si(111) where both AlGaN nanocolumns and the rough faceted matrix were observed. However, results from TEM analysis on this kind of samples showed that AlGaN nanocolumns nucleated on the AlN buffer surface (not on the AlGaN faceted matrix) *simultaneously* to the growth of the faceted matrix

The effect of AlN buffer on the targeted nanocolumnar morphology is shown in Fig. 10a and c that correspond to samples grown on AlN-buffered and bare Si(111) substrates, respectively,

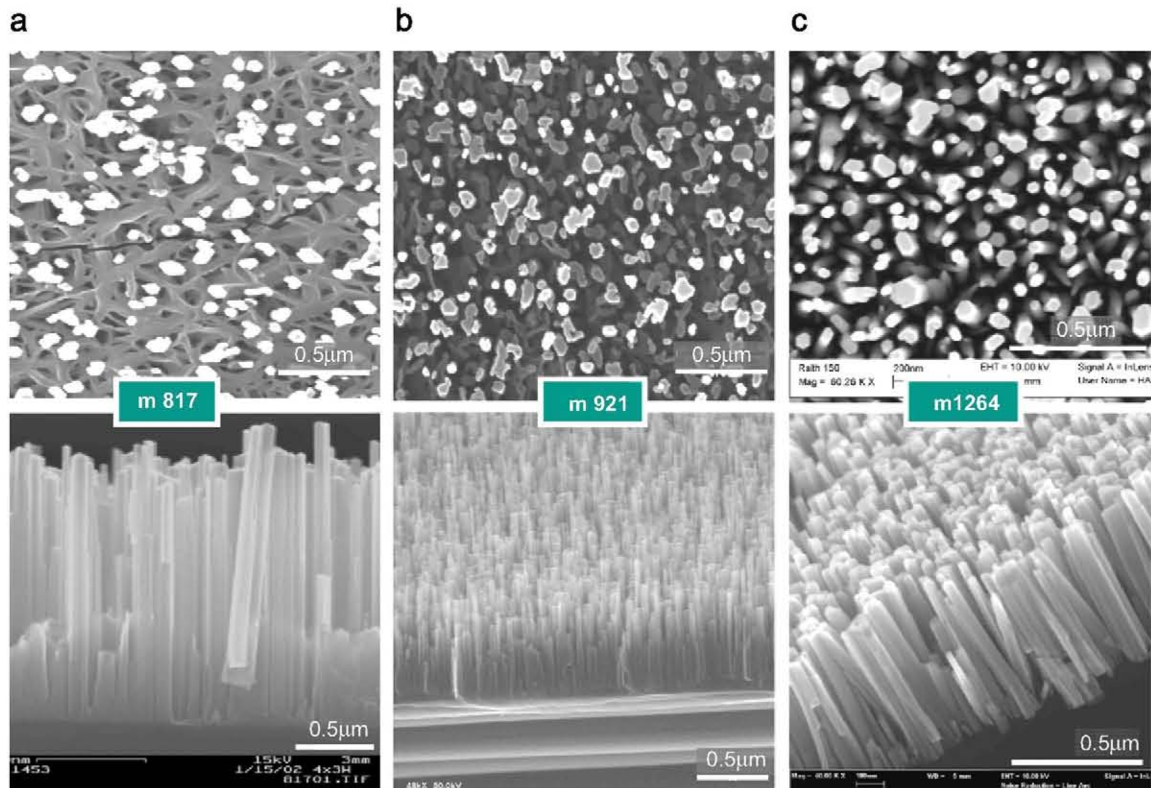

Fig. 10. Top and side SEM images of GaN nanocolumns grown at the same temperature on: (a) AlN buffered Si(111); (b) same AlN buffered Si(111) as in (a) with a higher nitrogen excess; and (c) bare Si(111) with the same III/V ratio as in (a).

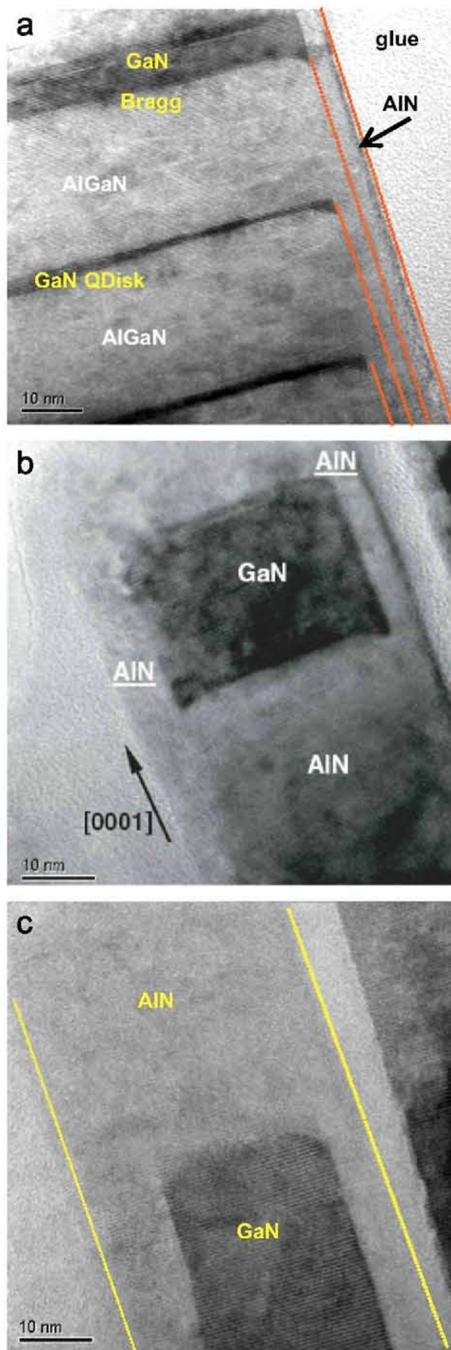

Fig. 12. HRTEM images of: (a) an AlGaN/GaN nanocolumnar heterostructure showing the enhancement of the lateral growth in Al-containing layers, as well as non-planar edges; (b) a nanocolumnar AlN/GaN Bragg reflector stack; and (c) an AlN nanocolumn grown on top of a GaN one under the same N-excess ((a) and (b) are from Ref. [31]).

lateral growth rate enhancement when growing AlN produces round-shaped edges, in agreement with the results reported in Ref. [31] and as illustrated in Fig. 12.

5. Conclusions

In the summary, a study of the spontaneous growth of GaN nanocolumns on Si(111) substrates by molecular beam epitaxy (MBE) has been presented. Results from the nanocolumnar growth on Ga droplet-patterned substrates clearly show that the growth mechanism is not the VLS, nor it requires any seeding or catalyst at the substrate surface. Instead, when present, Ga droplets may act as reservoirs that feed with Ga ad-atoms the neighbor nucleation sites and the nanocolumn growth, pointing to a kinetic process, where diffusion of Ga atoms towards the nanocolumn apex plays an important role.

The spontaneous nanocolumnar nucleation occurs most likely by a VW growth mechanism of small islands (of critical radius or larger than) driven by the lattice mismatch with the substrate, while the excess nitrogen reduces the lateral growth rate preventing the islands coalescence. Further nanocolumnar growth proceeds by Ga incorporation directly on the nanocolumn top and by Ga diffusion along the nanocolumn sidewalls up to its apex. The nanocolumns preserve their diameter during growth because of a very high metal ad-atom diffusion length on column sidewalls. However, an increase of the Ga flux may lead to Ga accumulation at the nanocolumn topmost region resulting in an enhancement of the lateral growth rate that increases of the nanocolumn top diameter. This effect may eventually lead to the nanocolumns merging in their upper regions.

When GaN nanocolumns are grown on AlN buffer, the lattice mismatch is drastically reduced. This lattice mismatch reduction can promote a SK or even a FM growth mode that yield wider islands that partially coalesce during the nucleation process (better wetting properties), resulting in a mixture of rough-compact material (faceted matrix) and nanocolumns. A smaller III/V ratio is needed to further reduce the metal-ad-atoms diffusion rate and to avoid the appearance of the faceted matrix.

In the case of nanocolumnar heterostructures with sequential GaN/Al(Ga)N layers, the Al-containing layers induce an increase of the nanocolumn diameter, together with a non-planar (faceted) edge growth of the subsequent layers. This effect may relate to a lower diffusion length of the Al ad-atoms on the nanocolumn sidewalls as compared to Ga ones. In this case, the increase of the nanocolumn diameter is not limited to the AlN region but also happens beyond the GaN/AlN heterojunction position along the nanocolumn sidewall. In addition, when the Ga flux is increased during the nanocolumn growth, the induced lateral growth rate enhancement, by metal accumulation, leads to the nanocolums top diameter enhancement and the eventual merging. The conclusions derived from this work may apply to other III-nitride nanocolumns grown on any substrate, with or without buffer layer.

Acknowledgments

J. Ristic would like to thank Prof. Benoit Deveaud-Pledran, Prof. Nicolas Grandjean, and Dr. Pascal Gallo for valuable scientific discussion. The authors wish to acknowledge partial support by the Spanish Ministry of Education and Science, Projects NAN2004-09109-C04-02; MAT2004-02875, Consolider CSD2006-00019, FIT-330100-2007-134, and by the CAM Project (IV PRICYT) S-0505/ESP-0200.

References

[1] M.A. Sánchez-García, E. Calleja, E. Monroy, F.J. Sánchez, F. Calle, E. Muñoz, R. Beresford, J. Crystal Growth 183 (1998) 23;
E. Calleja, M.A. Sánchez-García, F.J. Sánchez, F. Calle, F.B. Naranjo, E. Muñoz, S.I. Molina, A.M. Sánchez, F.J. Pacheco, R. García, J. Crystal. Growth 201 (1999) 296.

[2] M. Yoshizawa, A. Kikuchi, M. Mori, N. Fujita, K. Kushi, K. Kishino, Jpn. J. Appl. Phys. 36 (1997) L459.

[3] S. Guha, N. Bojarczuk, M. Johnson, J. Schetzina, Appl. Phys. Lett 75 (1999) 463.

[4] R. Calarco, M. Marso, T. Richter, A.I. Aykanat, R. Meijers, A.V. Hart, T. Stoica, H. Lüth, Nanoletters 5 (2005) 981.

K.A. Bertness, A. Roshko, N.A. Sanford, J.M. Barker, A.V. Davydov, J. Crystal Growth 287 (2006) 522.
R. Wagner, W. Ellis, Appl. Phys. Lett 4 (1964) 89.
M. Koguchi, H. Kakibayashi, M. Yazawa, K. Hiruma, T. Katsuyama, Jpn. J. Appl. Phys. 31 (1992) 2061.
W. Seifert, M. Borgström, K. Depperta, K.A. Dicka, J. Johansson, M.W. Larsson, T. Martensson, N. Skölda, C.P.T. Svensson, B.A. Wacaser, L.R. Wallenberg, L. Samuelson, J. Crystal Growth 272 (2004) 211.
K. Hiruma, M. Yazawa, T. Katsuyama, K. Ogawa, K. Haraguchi, M. Koguchi, H. Kakibayashi, J. Appl. Phys. 77 (1995) 447.
J.B. Hannon, S. Kodambaka, F.M. Ross, R.M. Tromp, Nature 440 (2006) 69.
E. Calleja, J. Ristić, S. Fernández-Garrido, L. Cerutti, M.A. Sánchez-García, J. Grandal, A. Trampert, U. Jahn, G. Sánchez, A. Griol, B. Sánchez, Phys. Stat. Sol. (b) 244 (2007) 2816.
E. Calleja, M.A. Sánchez-García, F.J. Sánchez, F. Calle, F.B. Naranjo, E. Muñoz, U. Jahn, K.H. Ploog, Phys. Rev. B 62 (2000) 16826.
One ML of Ga corresponds to exposure to the amount of Ga that would result in 1 ML thick GaN under stoichiometric growth conditions ($c/2 = 0.259$ nm).
H. Luth, Surfaces and Interfaces of Solid Materials, Springer, Berlin, 1993.
K.A. Bertness, A. Roshko, L.M. Mansfield, T.E. Harvey, N.A. Sanford, J. Crystal Growth 300 (2007) 94.
R.K. Debnath, R. Meijers, T. Richter, T. Stoica, R. Calarco, H. Lüth, Appl. Phys Lett 90 (2007) 123117.
B. Daudin, F. Widmann, G. Feuillet, Y. Samson, M. Arlery, J.L. Rouviere, Phys. Rev. B 56 (1997) R7069;
N. Gogneau, D. Jalabert, E. Monroy, T. Shibata, M. Tanaka, B. Daudin, J. Appl. Phys. 94 (2003) 2254.
R. Calarco, R.J. Meijers, R.K. Debnath, T. Stoica, E. Sutter, H. Lüth, Nanoletters 7 (2007) 2248.
K. Chopra, Thin Film Phenomena, McGraw-Hill, New York, 1969.
T. Zywietz, J. Neugebauer, M. Sheffler, Appl. Phys. Lett. 73 (1998) 487;
T. Zywietz, J. Neugebauer, M. Scheffler, J. Northrup, Chris G. Van de Walle, MRS Internet J. Nitride Semicond. Res. 3 (1998) 26.
V.A. Shchukin, N.N. Ledentsov, P.S. Kopev, D. Bimberg, Phys. Rev. Lett 75 (1995) 2968.
V.A. Shchukin, D. Bimberg, Rev. Mod. Phys. 71 (1999) 1125.
I. Daruka, A.-L. Barabasi, Phys. Rev. Lett 79 (1997) 3708.
A. Kikuchi, M. Kawai, M. Tada, K. Kishino, Jap. J. Appl. Phys. 43 (2004) L1524.
J. Northrup, J. Neugebauer, Phys Rev. B 53 (1996) R10477.
J. Elsner, M. Haugk, G. Jungnickel, Th. Frauenheim, Solid State Commun. 106 (1998) 739.
K. Rapcewicz, M. Buongiorno Nardelli, J. Bernholc, Phys. Rev. B 56 (1997) R12 725.
B. Daudin, G. Mula, P. Peyla, Phys. Rev. B 61 (2000) 10330.
J. Ristic, M.A. Sánchez-García, E. Calleja, J. Sánchez-Páramo, J.M. Calleja, U. Jahn, K.H. Ploog, Phys. Stat. Sol. (a) 192 (2002) 60;
J. Ristic, E. Calleja, M.A. Sánchez-García, J.M. Ulloa, J. Sánchez-Páramo, J.M. Calleja, U. Jahn, A. Trampert, K.H. Ploog, Phys. Rev. B 68 (2003) 125305.
A. Trampert, J. Ristic, U. Jahn, E. Calleja, K.H. Ploog, Conf. Ser, in: A.G. Cullis, P.A. Midgley (Eds.), Proceedings of the 13th International Conference on Microscopy of Semiconductor. Materials, vol. 180, IOP, 2003, p. 167.
J. Ristic, E. Calleja, A. Trampert, S. Fernández-Garrido, C. Rivera, U. Jahn, K.H. Ploog, Phys. Rev. Lett 94 (2005) 146102;
J. Ristić, E. Calleja, S. Fernández-Garrido, A. Trampert, U. Jahn, K.H. Ploog, M. Povoloskyi, A. Di Carlo, Phys. Stat. Sol. (a) 202 (2005) 367.
M. Tchernycheva, C. Sartel, G. Cirlin, L. Travers, G. Patriarche, J.-C. Harmand, Le Si Dang, J. Renard, B. Gayral, L. Nevou, F. Julien, Nanotechnology 18 (2007) 385306.